

Research



Cite this article: Chorro A, Verma B, Homfeldt M, Ibáñez B, Lawrence PA, Casal J. 2022 Planar cell polarity: intracellular asymmetry and supracellular gradients of Dachous. *Open Biol.* **12**: 220195.
<https://doi.org/10.1098/rsob.22.0195>

Received: 30 June 2022

Accepted: 21 September 2022

Subject Area:

developmental biology

Keywords:

asymmetry, planar cell polarity, Dach, Four-jointed, gradient, Fat

Authors for correspondence:

Peter A. Lawrence

e-mail: pal38@cam.ac.uk

José Casal

e-mail: jec85@cam.ac.uk

[†]These two authors contributed equally to this work.

[‡]Present address: Institut Jacques Monod, UMR 7592, Université Paris Cité / CNRS, Bâtiment Buffon, 15 rue Hélène Brion, 5205 Paris CEDEX 13, France.

[§]Present address: Department of Physiology, Anatomy and Genetics, Le Gros Clark Building, South Parks Road, University of Oxford, Oxford OX1 3QX, UK.

[¶]Present address: Hochschule Bremen, Biomimetics-Innovation-Centre, Neustadtswall 30, 28199 Bremen, Germany.

^{||}Present address: UICEC, Centro de Documentación Clínica Avanzada, Hospital Universitario Virgen del Rocío, Avd. Manuel Siurot s/n, 41013 Sevilla, Spain.

Electronic supplementary material is available online at <https://doi.org/10.6084/m9.figshare.c6238129>.

Planar cell polarity: intracellular asymmetry and supracellular gradients of Dachous

Adrià Chorro^{†,‡}, Bhavna Verma^{†,§}, Maylin Homfeldt[¶], Beatriz Ibáñez^{||}, Peter A. Lawrence and José Casal

Department of Zoology, University of Cambridge, Downing Street, Cambridge CB2 3EJ, UK

id PAL, 0000-0002-9554-8268; JC, 0000-0002-5149-1335

The slope of a supracellular molecular gradient has long been thought to orient and coordinate planar cell polarity (PCP). Here we demonstrate and measure that gradient. Dachous (Ds) is a conserved and elemental molecule of PCP; Ds forms intercellular bridges with another cadherin molecule, Fat (Ft), an interaction modulated by the Golgi protein Four-jointed (Fj). Using genetic mosaics and tagged Ds, we measure Ds *in vivo* in membranes of individual cells over a whole metamere of the *Drosophila* abdomen. We find as follows. (i) A supracellular gradient rises from head to tail in the anterior compartment (A) and then falls in the posterior compartment (P). (ii) There is more Ds in the front than the rear membranes of all cells in the A compartment, except that compartment's most anterior and most posterior cells. There is more Ds in the rear than in the front membranes of all cells of the P compartment. (iii) The loss of Fj removes intracellular asymmetry anteriorly in the segment and reduces it elsewhere. Additional experiments show that Fj makes PCP more robust. Using Dach (D) as a molecular indicator of polarity, we confirm that opposing gradients of PCP meet slightly out of register with compartment boundaries.

1. Background

1.1. A brief history of planar cell polarity

'We have, then, to imagine a system where the polarity of the cells depends on, or is, the direction of slope of a gradient.' [1]

'It is assumed that a concentration gradient exists between the frontal and the caudal margin of the segment. In *Galleria* the scales [...] orient in the direction of the steepest gradient.' [2]

Animals are largely constructed from epithelia and information about polarity within the epithelial plane is essential for organized development. For example, appendages must be built in the correct orientation, cilia must beat together in the right direction, vertebrate hairs and insect bristles must point accurately. This process must be coordinated as fields of cells usually share the same polarity. This property is referred to as planar cell polarity or PCP [3] and the mechanisms responsible for it have been investigated by transplantation, genetics, genetic mosaics, molecular biology and modelling.

The orientation of cells must relate to the developmental landscape; where is the head? where is the midline? Does this necessary information rely on a molecular device that, with reference to embryonic anatomy, points an arrow rather as a magnetic field orients a compass needle? If so, we would need to explain how polarity information is set up in relation to the main axes of the body, how it is conveyed to the cells and how it is read locally. Long ago, Lawrence [1] and Stumpf [2] proposed independently, on the basis of experimental results in different

insects, that the scalar values and slopes of morphogen gradients could provide both positional information and orienting information to the cells. A morphogen gradient was then imagined to be a supracellular concentration gradient of secreted molecules that is aligned to the axes of body or organ. The arrow of PCP would be a readout of the direction of slope of that gradient.

When research into PCP began [1–5], the genes responsible were not known but subsequently *Drosophila* genetics was applied to the problem, mutations that interfered with cell polarization were studied and several instrumental genes identified (e.g. [6,7]). Later, genes homologous to those in *Drosophila* were found in vertebrates and elsewhere and shown to be engaged in PCP. A nice example of this conservation is the stereocilia of the vertebrate inner ear whose exact orientation is critical for balance and hearing; attempts to analyse this process have been based on studies of PCP in the fruit fly [8].

Later, PCP genes were identified, sequenced and many have worked to understand what these proteins do. Genetic mosaics have proved to be a key method. Let's take an early and important example: mutations in the *frizzled* (*fz*) gene cause disturbance of PCP, but what happens if a small clone of cells that lack the gene are surrounded by normal cells? Gubb & Garcia-Bellido [9] found that although the *fz*⁻ clone itself produces disoriented hairs, several rows of the genetically normal cells surrounding the mutant patch were reoriented to point towards the clone, suggesting that cell interaction is a key element of the whole process.

From many years of research, it has become apparent that PCP is not directly but indirectly dependent on the slope of gradients of morphogens. Epithelial cells are oriented by gradients of other (PCP) molecules whose synthesis is regulated by and downstream of the morphogens themselves. Also, experiments have evidenced that there are two independent molecular systems of PCP; in both, cell interaction is an important component and each system can act alone to polarize cells. Both systems are independently oriented by morphogen gradients [10]. These two systems may act in support or in opposition to each other. Each of these systems depend on a specific set of molecules that form bridges between adjacent cells [10] (reviewed in [11–13]).

1.2. The Dachous/Fat system

Here we study one of these two molecular systems, the Ds/Ft system. Mutations affecting Ds and Ft cause misoriented cells. Their genes were found to specify large atypical proto-cadherin molecules. A Ft molecule in one cell is thought to bind to a Ds molecule in the other cell, thereby stabilizing both molecules in the cell membranes and forming a heterodimeric bridge from cell to cell [14,15]. Consequently, the accumulation of one molecule, say Ft, in a cell can affect the disposition of the other molecule, Ds, in the neighbouring cell—whose polarity may thus be altered, affecting the next neighbouring cell and so on [10].

The orientations of many cells are thought to be coordinated by one supracellular gradient of Ds activity. The shape of this gradient may be determined by not only the distribution of Ds protein itself but also, in the eye, by an opposing supracellular gradient of Fj [16]. Fj is a Golgi-resident kinase molecule that reduces the activity of Ds (in its binding to Ft) and increases the activity of Ft (in its binding to Ds) [17,18]. See figure 1 for a summary.

Yang *et al.* [19] made the first observations suggesting that, in the *Drosophila* eye, Ds and Fj are distributed in opposing gradients whose orientation relates to ommatidial polarity. Similarly, in the adult abdomen, Casal *et al.* [20] deduced from studying mutant clones and enhancer traps that, normally, Ds is graded in opposite directions in the A and P compartments and that Fj is also graded, but in the opposite sense to Ds, in both compartments. Evidence from enhancer traps and genetic mosaics have argued that both Ds and Fj are present in opposing gradients of function also in the eye and the wing [21,22] but we have no precise picture of the ranges, the shapes or the steepness of the gradients in any of these organs. There is an earlier molecular investigation of Ds in the abdominal metamere which indicates that there are gradients of amount [23]. We assess this data as supportive of gradients but preliminary—their quantitation does not measure the amount of Ds on single membranes (which we believe to be necessary) but records the distribution of Ds on joint membranes. No quantified data is provided and therefore the slope of any gradients remains unknown (see fig. 4 of their paper). Also, it was assumed that the boundaries of gradients are colinear with the lineage boundaries, which as we show below was not a correct assumption.

Evidence that the Ds/Ft system can drive PCP directly—and not via the Stan/Fz system, as had been proposed ([19,24], reviewed in [25])—came from experiments by Casal *et al.* [10] in the abdomen (reviewed in [26]). But that finding raised the question: how does it do so? We proposed that the numbers of bridges and their orientations (Ds-Ft or Ft-Ds) differed in amounts between the anterior and posterior membranes of each polarized cell (numbers that together determine the intracellular asymmetry). This molecular asymmetry within single cells was measured by Strutt's group but only in a small area of the wing disc near the peak of the gradient of Ds [27] and where the cells are strongly asymmetric in the localization of Dachs. Here we assess both the intracellular asymmetry and the supracellular gradient by measuring the amount of Ds of all single membranes over a whole metamere of the abdomen. We also study and analyse the effect of Fj on these parameters and explain its role in the Ds/Ft system itself. The abdomen was chosen as it is made up of atavistic segments rather than the wing or the eye which are appendages. Finally, and this is an important advantage, only in the abdomen is there a simple relationship between the axis of PCP (the hairs and denticles point posteriorly) and the main axis of the body (the anteroposterior axis).

2. Materials and methods

2.1. Mutations and transgenes

Flies were reared at 25°C on standard food. The FlyBase [28] entries for the mutant alleles and transgenes used in this work are the following:

hs.FLP: *Scer\FLP1^{hs,PS}*; *tub.Gal4*: *Scer\GAL4^{alphaTub84B}*; *UAS.nls-GFP*: *Avic\GFP^{UAS.Tag-MYC.Tag-NLS(SV40-largeT)}*; *tub.Gal80*: *Scer\GAL80^{alphaTub84B}*; *UAS.fz*: *fz^{Scer\UAS.c5a}*; *fj*: *fj¹*; *ds::EGFP*: *Avic\GFP^{ds-EGFP}*; *CycE*⁻: *CycE^{KG00239}*; *y⁺*: *Dp(1;2)sc¹⁹*; *w⁺*: *w^{+30c}*; *en.Gal4*: *Scer\GAL4^{en-e16E}*; *UAS.DsRed*: *Disc\RFP^{UAS.cKa}*; *hs.CD2*: *Rnor\Cd2^{hs.PI}*; *UAS.ft*: *ft^{UAS.cMa}*; *act>stop>d::EGFP*: *d^{FRT.Act5C.EGFP}*.

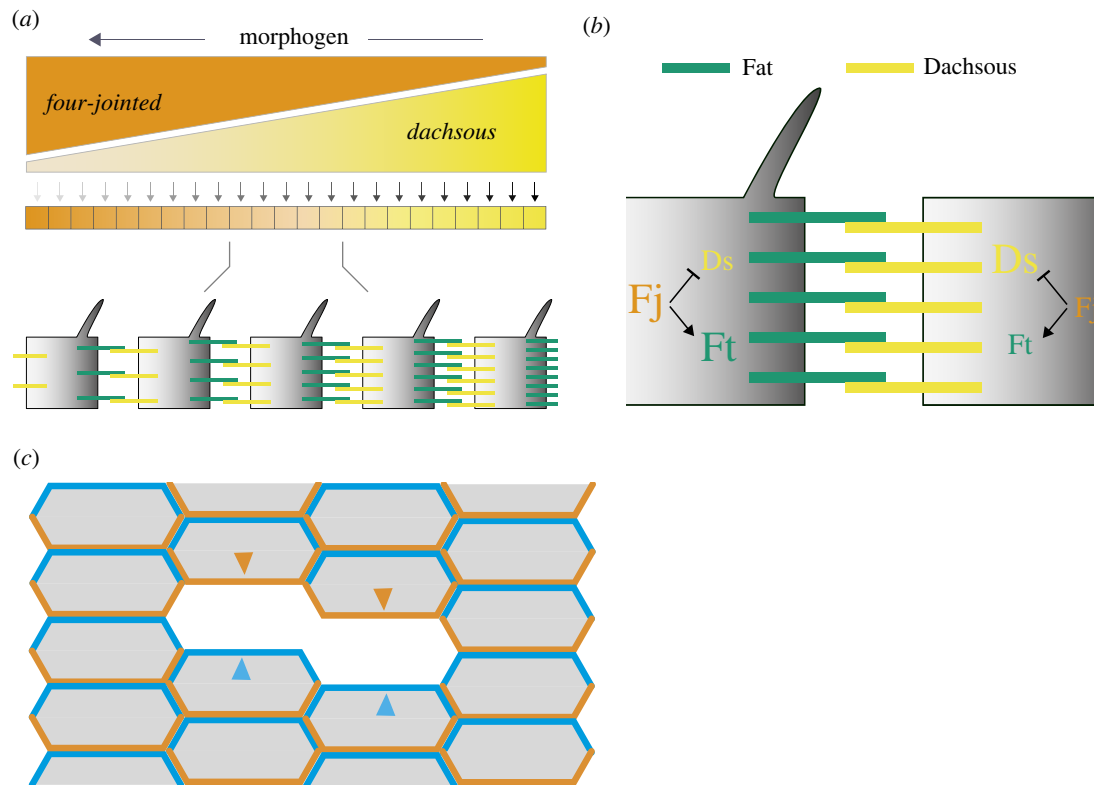


Figure 1. Model of the Ds/Ft system. (a,b) The anterior, or A compartment of a segment in the abdomen is shown. In response to gradient(s) of morphogen(s), opposing supracellular gradients of Fj and Ds are established. Fj predominates in the anterior region and Ds in the posterior region. Fj affects the binding of Ds with Ft and consequently both the Fj gradient and the gradient of Ds itself determine the distribution of Ds-Ft and Ft-Ds in the cells. A cell determines its polarity by comparing the disposition of Ft and/or Ds between its anterior and posterior membrane [10]. (c) How we isolate anterior or posterior membranes to measure tagged Ds in each. All the cells contain normal amounts of Ds, half of which is tagged. Tagged Ds is removed in small clones and replaced with normal untagged Ds. Consequently, the tagged Ds in only the posterior membrane (orange) or in only the anterior membrane (blue) of a cell flanking the clone can be measured.

2.2. Experimental genotypes

2.2.1. *UAS.fz* clones

y w hs.FLP tub.Gal4 UAS.nls-GFP / y w hs.FLP; FRT42D tub.Gal80/ FRT42D pwn; UAS.fz/ +

2.2.2. *UAS.fz* clones in ff^-

y w hs.FLP tub.Gal4 UAS.nls-GFP / y w hs.FLP; FRT42D tub.Gal80 ff^- / FRT42D pwn ff^- ; UAS.fz/ TM2

2.2.3. Untagged *ds* clones

y w hs.FLP; ds::EGFP CycE⁻ FRT40A / y⁺ w⁺ FRT40A en.Gal4 UAS.DsRed; +/- TM2

2.2.4. Untagged *ds* clones in ff^-

y w hs.FLP; ds::EGFP CycE⁻ FRT40A ff^- / y⁺ w⁺ FRT40A ff^- en.Gal4 UAS.DsRed

2.2.5. *UAS.ft* clones

y w hs.FLP/ w; FRT42D pwn / FRT42D tub.Gal80 hs.CD2; UAS.ft / tub.Gal4

2.2.6. *D::GFP* clones

y w hs.FLP/ w; +/- y⁺ w⁺ FRT40A en.Gal4 UAS.DsRed; act > stop > d::EGFP/ +

2.2.7. *D::GFP* clones in ff^-

y w hs.FLP/ w; ff^- / y⁺ w⁺ FRT40A ff^- en.Gal4 UAS.DsRed; act > stop > d::EGFP/ +

2.3. Cuticle clones

To induce clones overexpressing *fz* or *ft*, pupae of the appropriate genotypes were heat shocked, at 96–120 h after egg deposition, at 37°C for 30 min in a water bath. Between 2 and 3 days after eclosion, adult flies were selected and kept in tubes containing 70% ethanol. Cuticles were dissected and mounted in Hoyers medium. Images were taken on a Zeiss Axiophot microscope (Carl Zeiss Ltd, Cambourne, UK) equipped with Nomarski optics using a 40x/0.90 Plan-Neofluar lens, a Nikon D-300 camera (Nikon UK Ltd, Surbiton, UK) connected to an iMac computer and Nikon Camera Control Pro 2. Stacks of images taken at different focal planes were combined into a single image with Helicon Focus (HeliconSoft, Kharkiv, Ukraine).

2.4. Quantification of polarization strength

Overlapping images of adult cuticles containing overexpressing *fz* clones, labelled with *pawn*, were stitched together using Adobe Photoshop with the object of including the whole pigmented and haired area of the A compartment in a single image that was saved as a TIFF file. The file was opened with the ImageJ bundle Fiji. The segmented line tool was used to estimate the size of the A compartment

using pigmentation and hairs as landmarks [29], to measure the average distance between the anterior boundary of the A compartment and the anterior border of the clone, and the average length of the cuticle anterior to the clone that showed reversed polarization. Due to the irregular shape of the clones, the measurements were done at three different positions for each clone and the resultant average was used for the final plot. Note that for clones in the anterior (a2 region, [29]) of the A compartment, measurement of effect was limited, not by the extent of repolarization but by the lack of hairs in the a1 region. Therefore, clones close to the anterior boundary of hairs were not scored.

2.5. Live imaging of pupal epidermis

To induce clones expressing *ds::GFP* or untagged *ds* clones, pupae of the appropriate genotypes were heat shocked at 24 h after puparium formation at 33°C for 5 or 15 min, respectively, in a water bath. Twenty-four hours later, a 2 × 2 cm spacer was prepared with seven layers of double-sided tape (Tesafix 4964, Tesa UK Ltd., Milton Keynes, UK), and a hole 6 mm in diameter was punched out of the centre; the spacer was attached to a microscope slide. Each pupa was removed from the puparium, transferred to the hole with its dorsal side facing up, covered with Voltalef 10S oil (VWR International, Lutterworth, UK) and sealed with a coverslip. Epidermal cells in the A3–A5 abdominal segments of the pupa were imaged live using a Leica SP5 inverted confocal microscope with a 63×/1.4 oil immersion objective. Tagged fluorescent proteins were excited sequentially with 488 nm and 561 nm laser beams and detected with 500–540 nm and 570–630 nm emission filters, using Leica HyD hybrid detectors. To maximize the dynamic range and avoid clipping, the pixel depth was set to 12 bits and the gain and laser power were adjusted appropriately. Stacks of 1024 × 1024 pixel images were thus acquired.

2.6. Quantification of Dachsaus

Image stacks were opened in Fiji and projected into a single image with the Maximum Intensity Projection algorithm. Background was subtracted with a Rolling Ball of 6 pixels. The coordinates of the A/P and P/A boundaries (determined by the limits of *engrailed* expression) were obtained, as well of the average fluorescence intensity of the Ds signal in a 40 × 15 pixel box situated in a posterior region of the A compartment free of clones and abutting the A/P compartment boundary. Using the Freehand tool with a 6 pixel width, we measured the intensity of the Ds signal at the posterior and anterior border of untagged Ds clones (i.e. the intensity of the signal originated from a single anterior or posterior cell membrane, which may have variable numbers of puncta [14,27,30], figure 1c), recording the average of the intensity of three separate measures. Potentially confounding twin clones carrying two doses of *ds::EGFP* are absent as they were made homozygous for a *Cyclin E* lethal mutation [31]. The coordinates of the centre of each freehand line were also obtained, allowing us to determine the position of the clone borders relative to the length (in the anteroposterior axis) of the A or P compartments. Each fluorescence intensity was standardized (*relative intensity*) with respect to the intensity of the 40 × 15 pixel box measured before, and finally the *relative levels* used in the plots were calculated as $\log(\text{relative intensity}) - 3$. Percentage difference of Ds accumulation between compartment borders or between

anterior and posterior membranes was calculated using the formula $\text{percentage difference} = |(a - b)/((a + b)/2)| \times 100$, where *a* and *b* are relative levels.

2.7. Statistics and plotting

We used RStudio with R v.4.1.2 [32], and the *tidyverse* [33] and *mgcv* [34] packages.

3. Results

There are several interrelated projects:

1. We measure the differences in Ds amounts on opposite sides of individual diploid cells (histoblasts) across the whole abdominal metamere of the living pupa. This same data tells us also how the amount of membranous Ds varies across an entire segment, each segment comprising one A and one P compartment.
2. We study the contribution of Fj to the Ds/Ft system with respect to the metameres.
3. We map the molecular polarity of every cell in a segment using Dachs.

Here we use a fluorescent tag inserted into the endogenous Ds gene that does not affect function and the gene is normally regulated [27]. To measure the tagged Ds in any one cell membrane that protein must be singled out from any fluorescent signal contributed by the abutting membrane of a neighbour cell—this is achieved by making many patches (clones) of cells that contain only untagged Ds, thereby isolating single membranes bearing tagged Ds that face the periphery of these clones (see Material and Methods, figure 1c and electronic supplementary material, figure S1).

3.1. Supracellular distribution of Dachsaus across an abdominal metamere

In a single metamere of the pupal abdomen, about 37 cells were counted along the anteroposterior axis from front to back of the A compartment and about 11 cells spanned the P compartment (all cell divisions having stopped by this stage).

To find the distribution of Ds, we sampled along the anteroposterior axis; these numbers are then plotted against segment length. We report a supracellular gradient in the A compartment in which Ds increases in amount towards the rear as predicted ([10,20], see also [23]); a quasi-linear correlation is clearly seen and is robust and statistically significant (figure 2a, electronic supplementary material, figure S2). We find that the Ds gradient rises steadily in relative levels from 1.5 to 1.8 (ca 18% difference between its anterior and posterior limits). This quantitation confirms that the supracellular gradient of Ds in the P compartment is reversed, from a relative level of 1.8 at its anterior limit to 1.6 at the posterior limit, ca 10% difference (figure 2a, electronic supplementary material, figure S2).

3.2. Cellular asymmetry measured across an abdominal metamere

The results are shown (figure 2b; electronic supplementary material, figures S3 and S4). The data for the anterior and

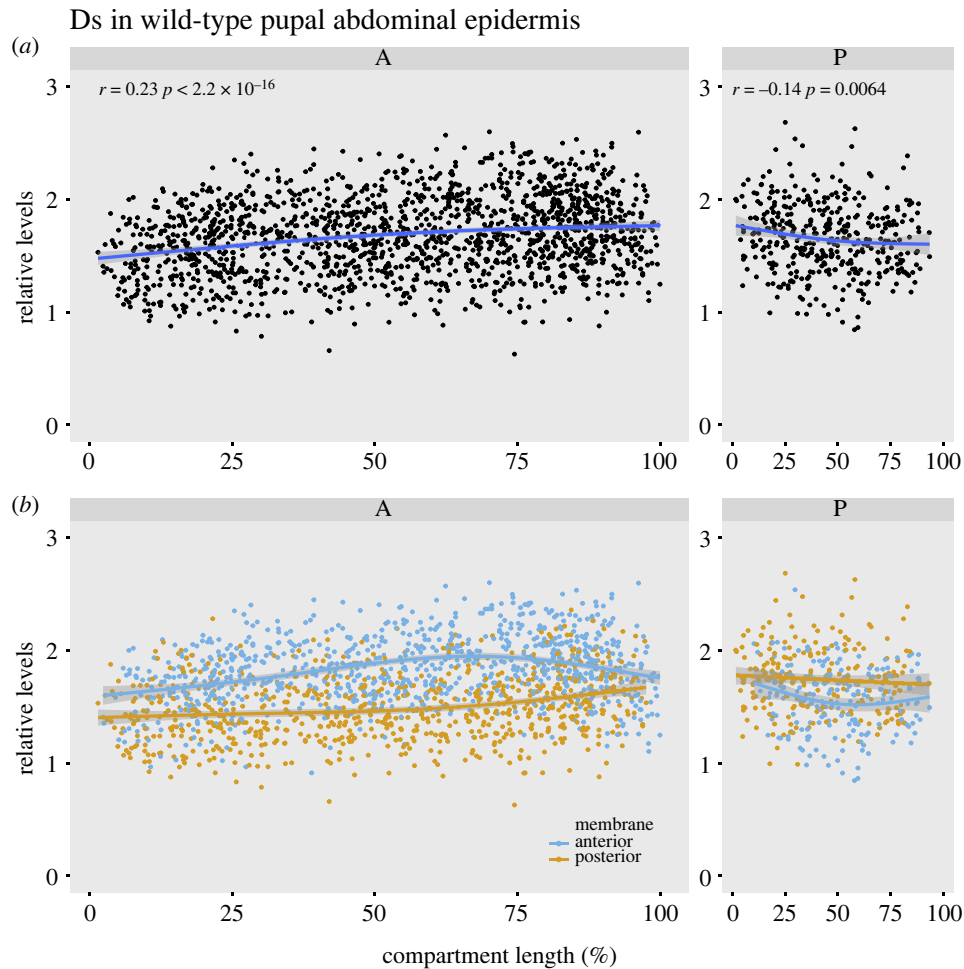


Figure 2. The supracellular gradient and cellular asymmetry of Ds in wild-type pupal epidermis. (a) Smoothed conditional means plots. All the measurements of Ds (both anterior and posterior cell membranes) are plotted across an entire metamere (0–100% of compartment length). A and P compartments are shown separately. The position of the compartment boundary was determined by mapping the expression of *engrailed*. The Pearson correlation coefficient was calculated. Supracellular gradients rise from the front to the back. There is a difference of 30% in relative levels in the A compartment, and 15% in the P compartment (where a is one limit and b the other: $100 \times (a - b) / ((a + b) / 2)$). The shaded area represents the 95% confidence interval for the fitted curve. (b) The data points from (a) are separated into anterior (blue) and posterior membranes (orange). Note both sets of data are graded but differ consistently in the relative Ds levels. In the A compartment, the amount of Ds is greatest in the anterior membranes (peaking near the middle of the compartment). In the P compartment, the amount Ds is greatest in the posterior membranes.

posterior membranes are plotted separately. As predicted [10], within the A compartment the anterior membranes contain more Ds than the posterior although the relative levels change across the segment. In the P compartment, there is cellular asymmetry also but with the opposite sign (high in the posterior membrane, as expected). In the P compartment, this asymmetry is statistically secure only in the central region located away from the A/P and P/A borders.

The maximum difference of relative levels of Ds between the anterior and posterior membranes occurs in the middle of each compartment being *ca* 27% in the A compartment and *ca* 13% in the P (figure 2b; electronic supplementary material, figures S3 and S4).

3.3. Cellular asymmetry and supracellular gradients in the absence of Four-jointed

Fj is clearly part of the Ds/Ft system, but the loss of Fj causes only slight effects on the wild-type phenotype. Nevertheless, comparing ff^+ and ff^- genotypes of the A compartment we find that the cellular asymmetry is significantly reduced relative to wild-type, most clearly in the anterior 20% of the A compartment (compare figures 2b and 3b; see also electronic

supplementary material, figures S3 and S4). A superposition of the data from both genotypes shows that, remarkably, the accumulation of Ds in the anterior membranes is not detectably affected by the removal of Fj (figure 3c). However, the relative levels of Ds recorded on posterior membranes of the cells are decreased in ff^- as compared to the wild-type (figure 3c). The same comparison in the P compartment (where, compared with the A compartment, the gradient and cellular asymmetry are reversed) shows that the loss of Fj has its largest effect on the anterior membranes (figure 3c).

Note that the supracellular gradients of both wild-type and ff^- differ little but there appears to be some reduction in the Ds gradient in ff^- , again in the most anterior region of the A compartment (compare figures 2a and 3a).

3.4. Estimating the effects of Four-jointed on the robustness of the Dachsous/Fat system

Even though the loss of Fj mainly affects the phenotype of the legs, the Fj protein may still have an important function in the abdomen. It could be that Fj makes the Ds/Ft system more robust, and this is evidenced by a reduction in the asymmetric distribution of Ds in the cellular membranes of ff^-

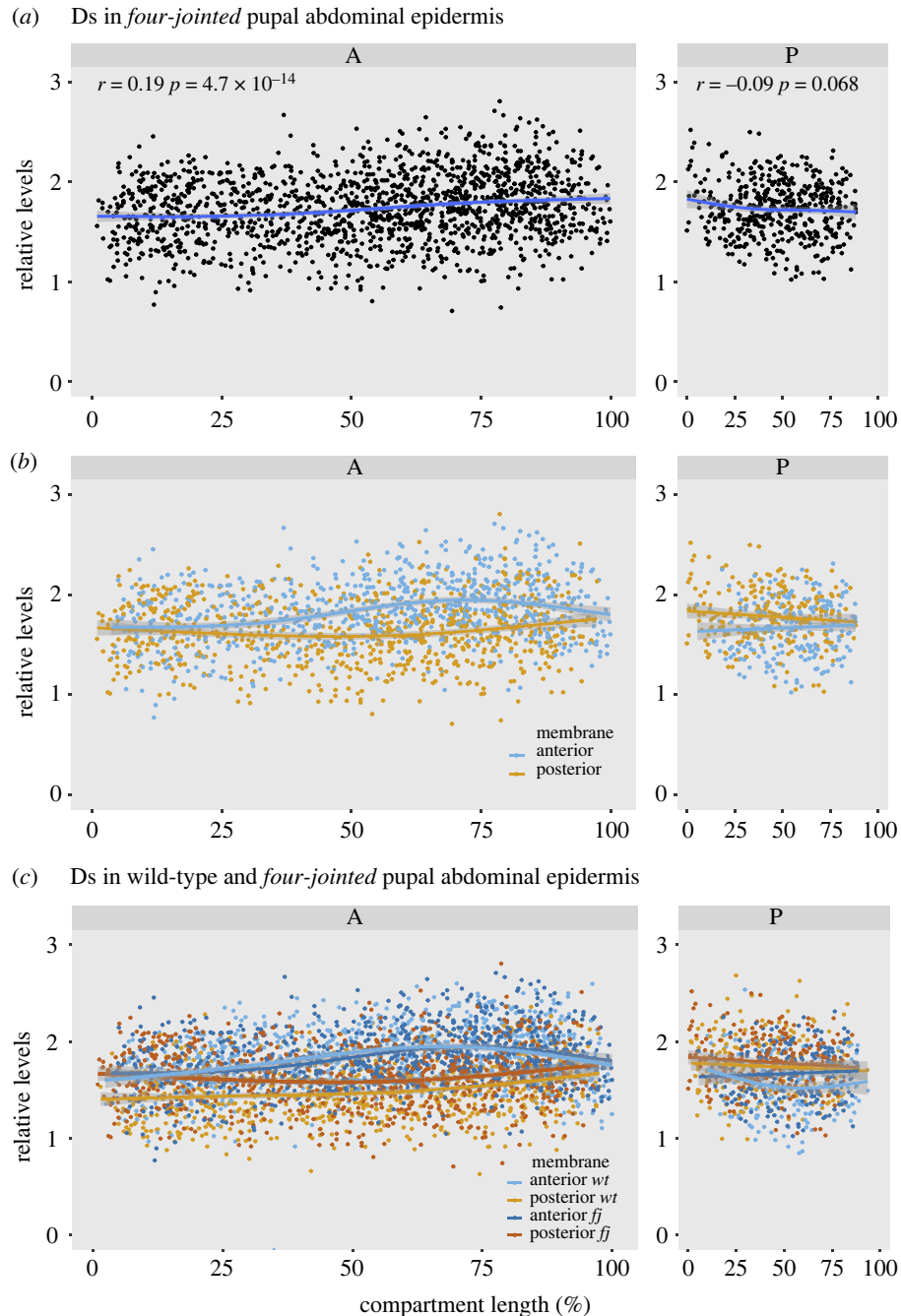


Figure 3. The supracellular gradient and cellular asymmetry of Ds in *fj*⁻ pupal epidermis. (a) and (b) compare with data shown in figure 2, the gradients are similar but somewhat shallower. In (b) note the loss of cellular asymmetry in the anterior region of the A compartment. (c) The wild-type and *fj*⁻ cell asymmetry data are both shown on one plot. The anterior membranes, in both A and P compartments, have similar values in both wild-type and *fj*⁻. Note that, in the A compartment of *fj*⁻ pupae, there is less Ds on the posterior membranes than in the wild-type, reducing the cellular asymmetry everywhere but especially in the anterior region (see also electronic supplementary material, figure S2).

cells (see above). This hypothesis can be tested: we employ the Stan/Fz system to reverse polarity locally within the A compartment and to succeed it must overcome the Ds/Ft system (which is trying to maintain normal polarity). Thus, the more robust the Ds/Ft system is, the better it will be able to resist and reduce the polarizing effects of the Stan/Fz system. We make small marked clones overexpressing *fz*, a key component of the Stan/Fz system; these cause all the cells around to point their hairs away from the clones, an effect only readily apparent in those areas anterior to those clones [35]. Comparing the polarity effects of *fz*-expressing clones in various positions in the anteroposterior axis, one sees no clear trend in wild-type flies. However, the local reversal of the polarity of bristles spreads much further in a

fj⁻ background, notably in the anterior region (figure 4). These findings argue that Fj strengthens the robustness of the Ds/Ft system, particularly at the front of the A compartment. This makes sense as there is independent but indirect evidence that, in the wild-type, the amount of Fj is graded within each segment, with the highest amount anteriorly where *fj*⁻ clones show the strongest phenotype [20,21].

3.5. Using Dachs to map cellular asymmetry throughout the pupal segment in *fj*⁺ and *fj*⁻ flies

The plots of Ds distribution (figure 2) showed that the cellular asymmetries dwindle and cross over near the A/P and P/

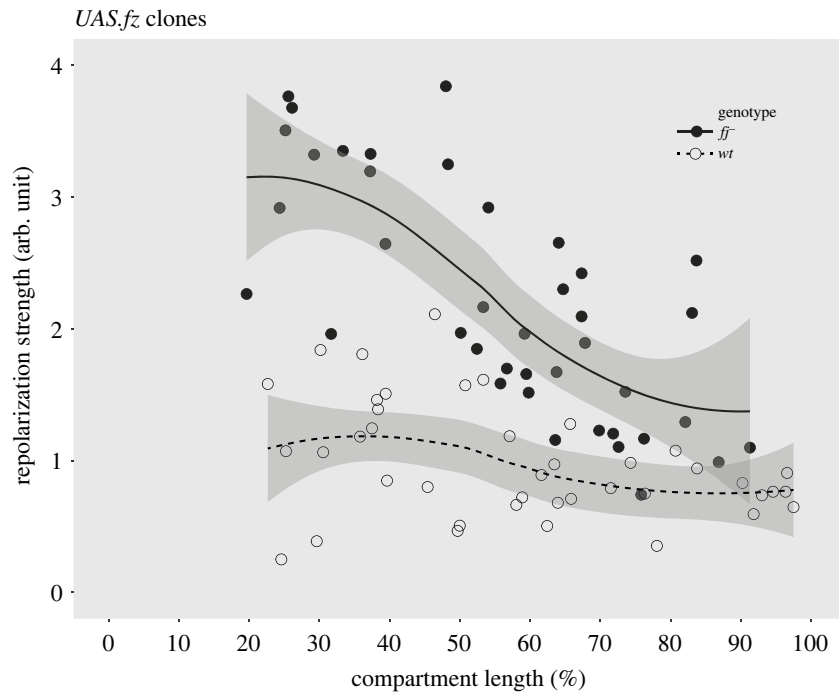


Figure 4. Estimating the robustness of the Ds/Ft system in the A compartment. Clones overexpressing *fz* reverse polarity anterior to the clone and they do so by overcoming the Ds/Ft system. In wild-type pupae, the extent of reversal is more or less uniform within the A compartment. However, in the absence of Fj, the Ds/Ft system is weakened in the anterior regions as shown by increased range of reversal when compared to wild-type (the shaded area represents the 95% confidence interval for the fitted curve).

A borders. These plots do not show exactly where the two opposing gradients meet and raise uncertainty as to where the cell polarity reverses. Dachs (D) protein is an excellent indicator of the polarity of the Ds/Ft system [36–38]. D is located on the membrane of the cell with the most Ds and this polarity may or may not correlate with other indicators, such as the pointing of adult hairs in the P compartment [23,39]. Given that we find most of the A compartment has a Ds gradient increasing posteriorly, are all the cells of the A compartment polarized appropriately? Note that, according to current models, D localizes at the membrane where Ds is in excess [37] and therefore should be localized anteriorly in the A compartment [10]. Given that most of the P compartment has the opposite gradient, do all the cells of the P compartment have D localized posteriorly? D localization is reported to switch from anterior to posterior polarity where the A and P compartments meet [23,39]. We now re-examine the distribution of D in the pupal abdomen of both wild-type and *ff⁻* flies, using small clones carrying tagged D in a background in which none of the D is tagged. In many cells, it is obvious whether D accumulates mainly or only on the anterior or posterior side. The results show that in the wild-type, in *most* of the A compartment D is found in the anterior membrane (figure 5*a*) and in *every* cell of the P compartment D is located in the posterior membrane (figure 5*b*). Within the A compartment, about two rows of the most anterior cells (figure 5*c*) and about two rows of the most posterior cells (figure 5*d*) show D located posteriorly; thus, their Ds/Ft polarity is that normally characteristic of the P cells. The third instar larva, having fewer but larger polyploid cells told a similar story: a set of cells in the A compartment, those confined to the extreme posterior row, had variable polarity with some showing the same polarity as in the P compartment (D accumulating posteriorly, [40]).

These findings place alternating fields of polarity out of register with the corresponding compartments and raise

questions about the role of the compartment boundary in the genesis of polarity [20]. We therefore decided to make polarity-changing clones that overexpress *ft* in order to alter polarity near compartment boundaries. Normally such *ft*-expressing clones will reverse the polarity of surrounding cells depending on the compartment (hairs point away from the clone in the A compartment and towards it in the P) [20]. One might expect a *ft*-expressing clone located posteriorly in the A compartment and touching the compartment boundary to behave like a normal A clone at the front and reverse the polarity of wild-type cells in front of the clone, and it does so (the wild-type hairs anterior to the clone now pointing away from the clone; figure 6*a*). One would expect that such a clone would meet P cells at its posterior edge and reverse the hairs behind the clone, and it does so (the wild-type hairs posterior to the clone now pointing towards the clone; figure 6*a*). Correspondingly, one would expect that a clone located at the front of the P compartment and contacting the A/P boundary to reverse both at front and behind, but it fails to reverse hairs in front (figure 6*b*). The explanation for both types of clones is simple: because the line of polarity reversal lies anterior to the lineage boundary, an A clone contacts A cells in front of it and P cells behind. However, the anterior extension of a P clone will be stopped at the A/P boundary and cannot reach the line of polarity reversal (thus it contacts cells behaving as P cells in front and therefore cannot reverse their polarity; figure 6*c*).

In the flies lacking Fj, unlike in the wild-type, many cells in the anterior region of the segment show reduced polarity, with D being distributed evenly around the cell membrane or at the posterior membrane (electronic supplementary material, figure S5). We think this finding correlates with our observation (above) that the most anterior region of the segment is where the robustness of the Ds/Ft system is most dependent on Fj. It is also pertinent that cells in the anterior region of the segment show loss of Ds asymmetry when Fj is removed (figure 3*b*). It also

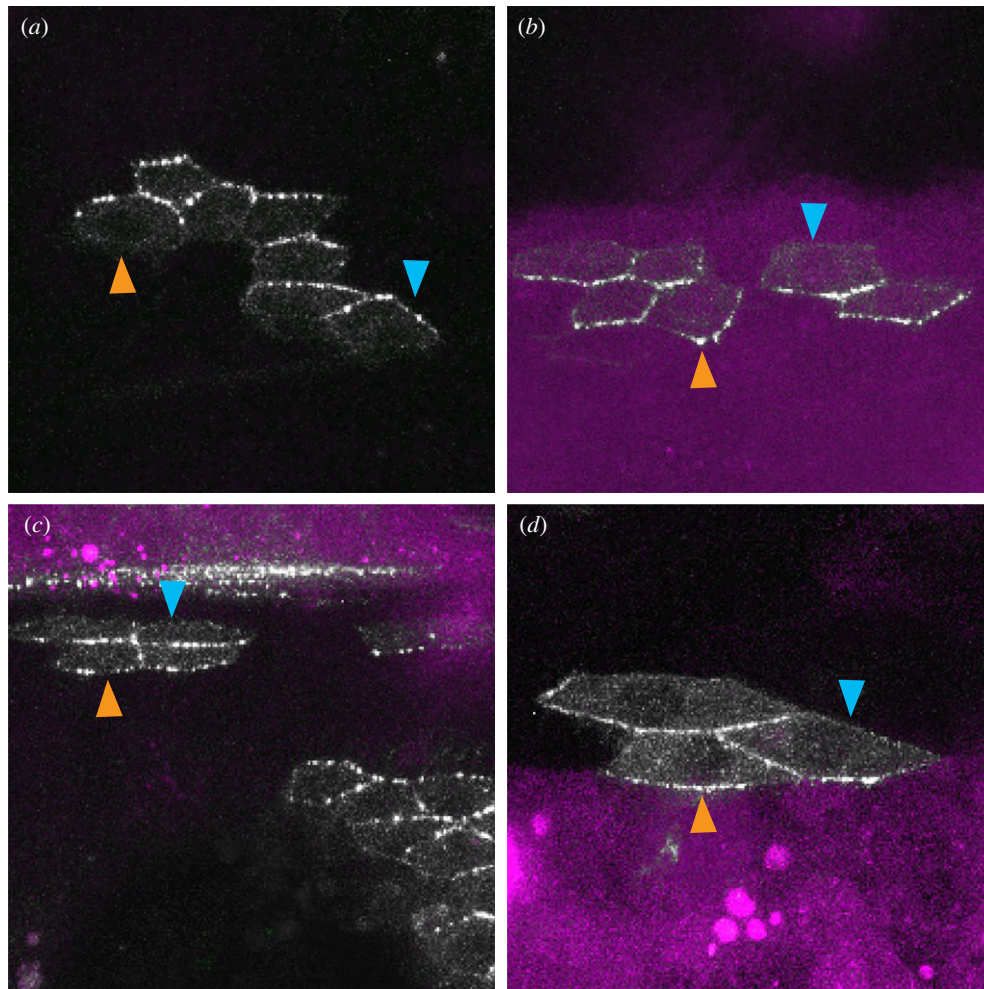


Figure 5. Asymmetric localization of Dachsh vis-à-vis A/P boundary. The areas shown are largely covered with clones lacking tagged D. We see from islands of cells containing tagged D that D is located anterior in most cells of the A compartment (*a*) and located posterior in cells of the P compartment (*b*). But that just within the A compartment, both near the anterior (*c*) and posterior limits (*d*), 1 or 2 rows of cells evince a polarity characteristic of P cells, with D located mainly on the posterior edges of the cells. The A/P boundary is demarcated by the anterior edge of *engrailed* expression that labels all cells of the P compartment (purple territory). Evidential membranes are marked with arrowheads, blue for anterior membranes and beige for posterior.

fits with the slight abdominal phenotype observed in *ff*⁻ flies, in which there was some loss of normal polarity but only in the anterior region of the segment [20,21]. Thus, all these findings point to the same conclusion: in cells of the anterior region of the segment, the polarization by the Ds/Ft system depends more on a gradient of Fj and less on a gradient of Ds—while in the middle and rear of the A compartment, the opposite is the case.

4. Discussion

Here we take the familiar model system of the *Drosophila* abdomen, in this case at the pupal stage, and measure the distribution of Dachshous (Ds) in the membranes of cells *in vivo*. We describe the intercellular gradients and intracellular asymmetry across a whole metamere. Ds is distributed in a gradient which is reflexed, rising in one direction in the A compartment of each metamere and falling in the P compartment (figure 2*a*). Although this pattern resembles that of a morphogen, our view is that Ds/Ft is not a morphogen: the primary function of a morphogen is to provide positional information to the cells in its field (reviewed in [41,42]), while the immediate purpose of the Ds/Ft gradient is to polarize cells. Also, and unlike an archetypal morphogen,

Ds does not move from cell to cell, although the numbers of Ds molecules in the membrane of one cell affect the distribution of Ft and Ds molecules in the adjacent cell [10]. There are models of how the Ds/Ft system works, how polarity information passes from cell to cell and how a gradient of Ds activity might point the arrow of polarity [10,13,30,43]. Our results validate the hypothesis that the orientation of molecular gradients determines the polarity of the cells [1,2].

The amount of Ds forms a linear gradient along the anteroposterior axis of the A compartment, resulting in a difference of about 18% between the anterior and posterior limits. We measure the cellular asymmetry in the distribution of Ds across the whole metamere. In the A compartment, it is higher in the anterior membrane of the cell than in the posterior membrane (as predicted [10]). In the P compartment, both the direction of slope of the gradient and its asymmetrical distribution in the cell are opposite to that in the A compartment [10]. The difference between anterior and posterior membranes is far less than that found when a small region of the wing imaginal disc was studied (twofold [27]). However, modelling predicted that the difference in the primordium of the wing disc could be less than twofold [30]. Are such differences sufficient to polarize individual cells? The answer is not known but certainly, as we have summarized in background, previous experiments argue that the

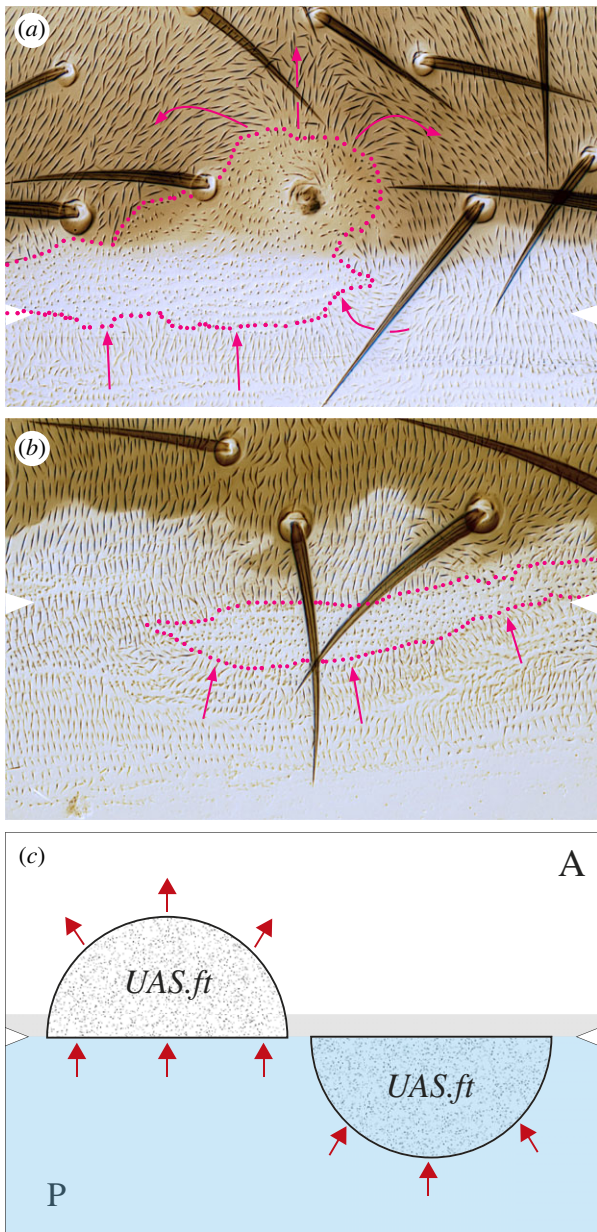


Figure 6. Clones overexpressing *ft* near the A/P compartment border. (a) Clone of A compartmental provenance reverses territory, red arrows, both in front (in A territory) and behind (in P territory). (b) Clone of P compartmental provenance reverses the polarity of cells behind (in P territory) but fails to reverse in front (A territory). White arrowheads show estimated position of A/P borders, red dots mark clone boundaries. (c) Simplified diagram of above results; note line of polarity reversal (defined by the line where the location of Dachs, a polarity indicator, changes) is situated anterior to the A/P boundary by 1–2 cells (defining a narrow zone, shaded), and this explains the outcomes, see text; these results mimic earlier ones with *ft*-overexpressing clones [20].

polarity of single cells is determined by the slope of a gradient. It is relevant that in *Dictyostelium*, where chemotaxis has been studied by many, the ability of single cells to read gradients with concentration differences of only 1–5% across the cell has been shown, implying that there are only about 5 more occupied receptors at the front than the back half of the cell [44–46].

4.1. The function of Four-jointed

There is considerable evidence from enhancer traps and from functional experiments that Fj forms a gradient [16,20,21].

In the A compartment of each abdominal segment, it is evidenced to be highest in the most anterior region [20]. Fj phosphorylates both Ds and Ft proteins [47], the effect on Ds is to decrease its affinity for Ft, while phosphorylated Ft has an increased affinity for Ds [17,18]. It is thought that the two opposing gradients, Ds and Fj, work together to produce asymmetric distributions of Ds-Ft bridges [10,18]. Most pertinently, Hale *et al.* [30] have used FRAP to investigate the stability of Ds-Ft heterodimers in the wing disc and observed differences between *ff*⁺ and *ff*⁻ flies. They concluded that ‘the overall result of removing Fj was a reduction in stability of the Ft-Ds dimer’. We cannot divine from this how the stability of bridges might impact on cell asymmetry in different parts of the abdominal segment. This is partly because Hale *et al.* look at the conjoined membranes of two cells while we distinguish anterior from posterior membranes of each cell. We do find that removing Fj increases the relative amount of Ds in the posterior membrane over much of the A compartment. Since Ds is stable in the membrane only when joined to Ft in the next cell [14], it follows there should be more bridges in *ff*⁻ segments. This conclusion does not fit easily the main finding of Hale *et al.* [30]. But they also deduced that the action of Fj on Ft dominated over its effect on Ds; however, that finding applied to their sample area (the wing pouch) which is near the top of the Fj gradient; they do not tell us what, if any, might be the function of Fj in areas where Ds expression is high but Fj low. Our data concern the whole field and argue that Fj is essential for cellular asymmetry in only the anterior part of the A compartment (where it peaks in the wild-type), but it is also needed in the rest of the compartment to achieve a robust cellular asymmetry.

Perhaps the most problematic fact about Fj is that removing it has little overt effect on phenotype. Nevertheless, in *ff*⁻ flies, we found changes in Ds distribution and a loss of robustness—shown by a reduction of the Ds/Ft system’s ability to resist polarity changes induced by clones in the Stan/Fz system. Strikingly, in the anterior *ca* 20% of the A compartment, the loss of Fj tends to totally depolarize the cells, eliminating the asymmetric localization of D. We conclude that the main function of Fj in the abdomen, via its action on Ds and Ft, is to strengthen the Ds/Ft system mainly at the front of the A compartment where Ft is high and Ds is low.

Another clear finding demands an explanation: when the localizations of Ds in the A compartments of *ff*⁺ and *ff*⁻ flies are compared, they differ considerably, but only in the posterior membranes of the cells (figure 3). It seems that Fj promotes the presence of Ds-Ft dimers more strongly in the posterior than in the anterior membranes. We offer a speculative model to explain this (figure 7).

4.2. The ranges of the Dachsous gradients

In order to map the polarity of all the cells individually, we looked at tagged D, whose asymmetric distribution depends on the localization of Ds and Ft in the cell [36,37]. We expected [20] (and it was even reported by others [23,39]) that this inflection of cell polarity as well as the limits of the Ds/Ft gradients would coincide at the A/P borders. However, our maps of D asymmetry make clear that the changeover of polarity occurs not at the compartment border but just within the A compartment—a result that at last makes sense of earlier findings with clones overexpressing *ft*. Generally in the A compartment,

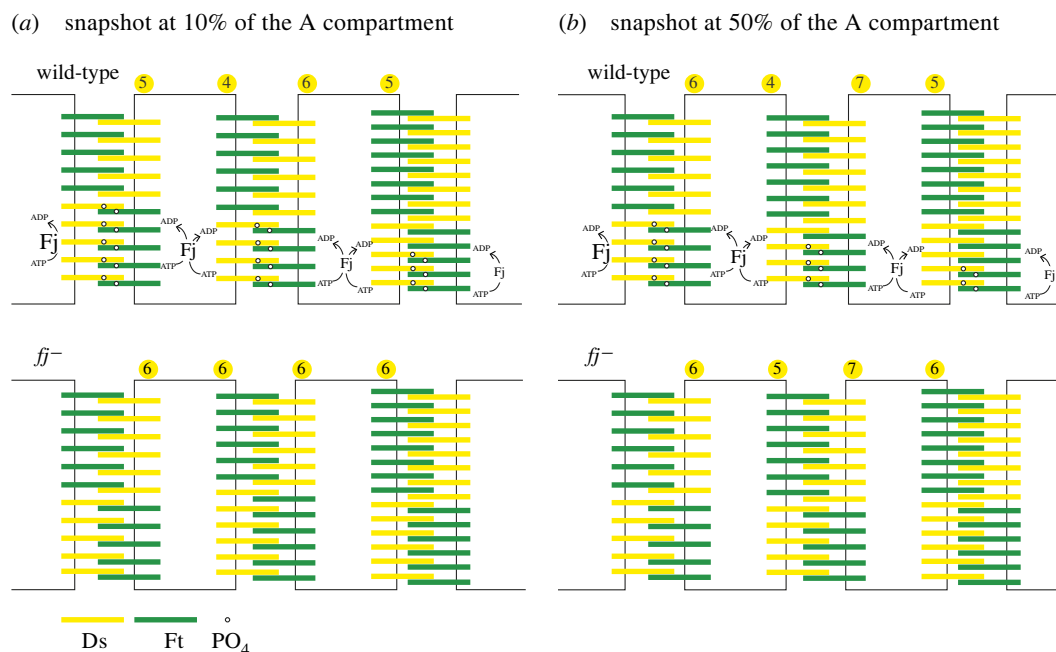


Figure 7. Speculative model of the action of Fj on Ds-Ft heterodimers. Why does the loss of Fj particularly affect the posterior membranes of cells? Two places in the A compartment are shown. (a) 10% back from the anterior limit of the A compartment. In this area, Fj is largely responsible for the supracellular gradient and cellular asymmetry. Phosphorylating Ds reduces its tendency to bind to Ft while phosphorylating Ft increases its tendency to bind to Ds [17,18]. The Ds phosphorylated by Fj is shown to be inserted preferentially into the posterior membrane (rather than into the anterior membrane). There it is less successful (than unphosphorylated Ds) in forming partners with Ft in the abutting cell and consequently less Ds accumulates in that membrane, leading to the cellular asymmetry of Ds found in this region of the wild-type (figure 3c). We don't know why this might be so; it is possible that phosphorylated Ds could be transported posteriorly in the cell. Below, the same location but in *ff*⁻ pupae. Cellular asymmetry is much weaker or absent and does not vary with position and the gradient is almost flat due to low levels of available Ds in this area because there is now no Fj to drive polarity by phosphorylating Ds. (b) 50% back from the anterior limit of the A compartment. In this area, the gradient of Ds is sufficient to drive both the supracellular gradient and the cellular asymmetry, thus, below, even in the absence of Fj, both the gradient and the asymmetry persist with only slight reduction in strength; mainly due to an increase in unphosphorylated Ds at posterior membranes. As in (a), we imagine phosphorylated Ds being added preferentially to the posterior membranes of cells.

hairs pointed away from the clones (suggesting a Ds gradient that rose from anterior to posterior), and in the P compartment, hairs pointed towards the clones (suggesting a Ds gradient that fell from anterior to posterior) [20]. However, the behaviour of some *ff*-expressing clones, those that contacted a compartment border, did not fit with our expectation at that time. For example, clones belonging to the P compartment that reached the very front edge of the P compartment should reverse the polarity of A cells in front but did not do so. Why not? We were flummoxed and offered an *ad hoc* explanation [20]. Now we know that cells at the extreme rear of the A compartment have the Ds/Ft polarity of P cells, a simpler explanation makes more sense (electronic supplementary material, figure S6). Because *ft* and *ff*-expressing clones in the P compartment are not able to extend across the compartment boundary to contact cells with normal A polarity, they must, as observed, continue to behave as P clones at their anterior margins because, although they confront cells of A lineage, those cells have the polarity of P cells. Consequently, effects on the disposition of bridges will reinforce, rather than alter, normal polarity.

This new picture recalls other effects of compartmental borders in fly development. An example is the A/P wing border. The interface between a signalling P and a receiving A compartment leads to a signal (Hedgehog) crossing over from P to A and initiating a response in the first cells of the receiving compartment (turning on Dpp expression [48,49]). We wonder if our finding relates to this: could a signal coming from the P compartment during early development initiate changes in the first cell row or two of the A

compartment that spread forwards and backwards from there to induce a reflexed Ds/Ft gradient in the A and the P compartment? It is relevant that [50] have argued that the Ds/Ft gradient might be initially aligned in the anteroposterior axis in the pupal wing (that is, orthogonal to hair orientation). In which case, a Ds/Ft gradient in the wing could also relate to a signal, such as Hedgehog, crossing over the boundary from the P compartment into A.

4.3. Steepness model and growth

In thinking about the control of growth, and many have done so, we should remember that it is likely to be complicated and multi-factorial. For example, regarding the role of the Ds/Ft system, the removal of either Ft or Ds breaks that system and yet the flies still grow. It follows that models relating to the Ds/Ft system such as the steepness hypothesis [51,52], or the feed-forward model of growth [53] may prove insufficient. Here we find that, within each compartment, the difference between anterior and posterior membranes is largely uniform and the supracellular gradient is largely linear. These are both prerequisites for the simplest steepness model. In order to draw the arrow of PCP, anterior and posterior membranes of a cell must be locally compared, and for this, there is indirect evidence [54]. We conjectured that, in addition, the degree of difference between these two cell membranes might feed into the decision as to whether a cell divides or dies [51] and help to limit growth. This would amount to a dimension-sensing mechanism. The steepness model is also supported by

experiments showing that interfaces between cells with different amounts of Ds lead to Hippo target genes being activated and increased local growth across that interface [55].

4.4. One or two systems?

We have argued that the Ds/Ft and Stan/Fz systems act independently [10,26] but this is not accepted by everyone [56]. Some authors have taken refuge in the postulate that PCP might operate differently in various organs, so the two systems might be independent in one organ (the abdomen) but are united in a single pathway of function in other organs (e.g. the wing) or that any direct action of Ds/Ft on cell polarization might constitute a 'bypass pathway' [22,56]. We view that refuge as intrinsically precarious. The many experiments and contrasting interpretations in this area are well presented by Strutt & Strutt [57]. The recent intervention of the *pk* gene into this mêlée has not simplified that debate [39,58–61]. However, our results above (those comparing *fz*-expressing clones in abdomens with and without Fj, figure 4, where we ask one PCP system to act against the other), are simply explained if the systems act independently. Under the alternative model, in which the Stan/Fz system is presumed to act downstream of the Ds/Ft system, explaining the differing effects of *fz*-expressing clones on polarity in *ff*⁺ and *ff*⁻ flies would tax the finest minds. Our opinion is that the two systems can function distinctly everywhere and act in conflict or in synergy. They interact late in the cellular process such as when hairs are being formed in their final orientations.

4.5. Some remaining questions

There are many outstanding questions about the Ds/Ft system. Does the amount of Ft vary over the field? What other factors, apart from Fj, modulate the interaction of Ds and Ft molecules? How exactly is the supracellular gradient read in order to orient polarity of cells? How are opposing membranes of a cell compared in order to polarize that cell? Ds and Ft proteins are together localized into puncta

[62] but why are they and are puncta required for proper function? We found the Ds/Ft gradient to be reflexed; consequently, since all the hairs point posteriorly, they must be pointing up the Ds gradient in nearly all of the A compartment and down the Ds gradient in the P compartment. How is this achieved? One simple hypothesis is that hair polarity is the outcome, in the A compartment, of both the Ds/Ft and the Stan/Fz systems instructing the hairs to point posteriorly. However, in the P compartment, the Ds/Ft system aims to point the hairs forward and the Stan/Fz aims to point backwards and, to put this too simply, the Stan/Fz system wins. The *prickle* gene also plays a part in this (see [39,57–60,63]).

Data accessibility. Data used in figures 2–4 and electronic supplementary material, figures S2–S4 can be obtained from the University of Cambridge Open Access repository: <https://doi.org/10.17863/CAM.85748> [64].

Supplementary material is available online [65].

Authors' contributions. A.C.: data curation, formal analysis, investigation, resources, validation and visualization; B.V.: data curation, formal analysis, investigation, resources, validation and visualization; M.H.: data curation, formal analysis, investigation, resources, validation and visualization; B.I.: data curation, formal analysis, investigation, resources, validation and visualization; P.A.L.: conceptualization, funding acquisition, investigation, methodology, project administration, supervision, visualization, writing—original draft and writing—review and editing; J.C.: conceptualization, data curation, formal analysis, investigation, methodology, resources, software, supervision, validation, visualization and writing—review and editing.

All authors gave final approval for publication and agreed to be held accountable for the work performed therein.

Conflict of interest declaration. We declare we have no competing interests.

Funding. Our work was supported by Wellcome Investigator Award 107060/Z/15/Z to P.A.L.

Acknowledgements. We thank David Strutt for his help, particularly the stock carrying the tagged Ds and advice, Malcolm Burrows and Gary Struhl for encouragement and the Wellcome Trust (four consecutive grants), the Zoology Department and the Newton Trust for supporting our experiments over the last 16 years. Stocks obtained from the Bloomington Drosophila Stock Center (NIH P40OD018537) were used in this study.

References

- Lawrence PA. 1966 Gradients in the insect segment: the orientation of hairs in the milkweed bug *Oncopeltus fasciatus*. *J. Exp. Biol.* **44**, 607–620. (doi:10.1242/jeb.44.3.607)
- Stumpf HF. 1966 Über gefälleabhängige Bildungen des Insektensegmentes. *J. Insect Physiol.* **12**, 601–617. (doi:10.1016/0022-1910(66)90098-9)
- Nübler-Jung K. 1979 Pattern stability in the insect segment. II. The intersegmental region. *Wilhelm Roux Arch. Dev. Biol.* **186**, 211–233. (doi:10.1007/BF00848590)
- Wigglesworth VB. 1940 Local and general factors in the development of 'pattern' in *Rhodnius prolixus* (Hemiptera). *J. Exp. Biol.* **17**, 180–201. (doi:10.1242/jeb.17.2.180)
- Piepho H. 1955 Über die polare Orientierung der Bälge und Schuppen auf dem Schmetterlingsrumpf. *Biol. Zbl.* **74**, 467–474.
- Adler PN. 1992 The genetic control of tissue polarity in *Drosophila*. *Bioessays* **14**, 735–741. (doi:10.1002/bies.950141103)
- Usui T, Shima Y, Shimada Y, Hirano S, Burgess RW, Schwarz TL, Takeichi M, Uemura T. 1999 Flamingo, a seven-pass transmembrane cadherin, regulates planar cell polarity under the control of Frizzled. *Cell* **98**, 585–595. (doi:10.1016/s0092-8674(00)80046-x)
- Jones C, Chen P. 2007 Planar cell polarity signaling in vertebrates. *Bioessays* **29**, 120–132. (doi:10.1002/bies.20526)
- Gubb D, Garcia-Bellido A. 1982 A genetic analysis of the determination of cuticular polarity during development in *Drosophila melanogaster*. *J. Embryol. Exp. Morphol.* **68**, 37–57.
- Casal J, Lawrence PA, Struhl G. 2006 Two separate molecular systems, Dachsous/Fat and Starry night/Frizzled, act independently to confer planar cell polarity. *Development* **133**, 4561–4572. (doi:10.1242/dev.02641)
- Carvajal-González JM, Mlodzik M. 2014 Mechanisms of planar cell polarity establishment in *Drosophila*. *F1000Prime Rep.* **6**, 98. (doi:10.12703/p6-98)
- Goodrich LV, Strutt D. 2011 Principles of planar polarity in animal development. *Development* **138**, 1877–1892. (doi:10.1242/dev.054080)
- Lawrence PA, Casal J. 2018 Planar cell polarity: two genetic systems use one mechanism to read gradients. *Development* **145**, dev168229. (doi:10.1242/dev.168229)
- Ma D, Yang CH, McNeill H, Simon MA, Axelrod JD. 2003 Fidelity in planar cell polarity signalling. *Nature* **421**, 543–547. (doi:10.1038/nature01366)
- Matakatsu H, Blair SS. 2004 Interactions between Fat and Dachsous and the regulation of planar cell

- polarity in the *Drosophila* wing. *Development* **131**, 3785–3794. (doi:10.1242/dev.01254)
16. Zeidler MP, Perrimon N, Strutt DJ. 1999 The Four-jointed gene is required in the *Drosophila* eye for ommatidial polarity specification. *Curr. Biol.* **9**, 1363–1372. (doi:10.1016/S0960-9822(00)80081-0)
 17. Brittle A, Repiso A, Casal J, Lawrence PA, Strutt D. 2010 Four-jointed modulates growth and planar polarity by reducing the affinity of Dachsous for Fat. *Curr. Biol.* **20**, 803–810. (doi:10.1016/j.cub.2010.03.056)
 18. Simon MA, Xu A, Ishikawa HO, Irvine KD. 2010 Modulation of Fat:Dachsous binding by the cadherin domain kinase Four-jointed. *Curr. Biol.* **20**, 811–817. (doi:10.1016/j.cub.2010.04.016)
 19. Yang CH, Axelrod JD, Simon MA. 2002 Regulation of Frizzled by Fat-like cadherins during planar polarity signaling in the *Drosophila* compound eye. *Cell* **108**, 675–688. (doi:10.1016/S0092-8674(02)00658-x)
 20. Casal J, Struhl G, Lawrence PA. 2002 Developmental compartments and planar polarity in *Drosophila*. *Curr. Biol.* **12**, 1189–1198. (doi:10.1016/S0960-9822(02)00974-0)
 21. Zeidler MP, Perrimon N, Strutt DJ. 2000 Multiple roles for Four-jointed in planar polarity and limb patterning. *Dev. Biol.* **228**, 181–196. (doi:10.1006/dbio.2000.9940)
 22. Simon MA. 2004 Planar cell polarity in the *Drosophila* eye is directed by graded Four-jointed and Dachsous expression. *Development* **131**, 6175–6184. (doi:10.1242/dev.01550)
 23. Mangione F, Martin-Blanco E. 2018 The Dachsous/Fat/Four-jointed pathway directs the uniform axial orientation of epithelial cells in the *Drosophila* abdomen. *Cell Rep.* **25**, 2836–2850. (doi:10.1016/j.celrep.2018.11.036)
 24. Adler PN, Charlton J, Liu J. 1998 Mutations in the cadherin superfamily member gene dachsous cause a tissue polarity phenotype by altering frizzled signaling. *Development* **125**, 959–968. (doi:10.1242/dev.125.5.959)
 25. Tree DR, Ma D, Axelrod JD. 2002 A three-tiered mechanism for regulation of planar cell polarity. *Semin. Cell Dev. Biol.* **13**, 217–224. (doi:10.1016/S1084-9521(02)00042-3)
 26. Lawrence PA, Struhl G, Casal J. 2007 Planar cell polarity: one or two pathways? *Nat. Rev. Genet.* **8**, 555–563. (doi:10.1038/nrg2125)
 27. Brittle A, Thomas C, Strutt D. 2012 Planar polarity specification through asymmetric subcellular localization of Fat and Dachsous. *Curr. Biol.* **22**, 907–914. (doi:10.1016/j.cub.2012.03.053)
 28. Gramates LS *et al.* 2022 FlyBase: a guided tour of highlighted features. *Genetics* **220**, iyac035. (doi:10.1093/genetics/iyac035)
 29. Struhl G, Barbash DA, Lawrence PA. 1997 Hedgehog organises the pattern and polarity of epidermal cells in the *Drosophila* abdomen. *Development* **124**, 2143–2154. (doi:10.1242/dev.124.11.2143)
 30. Hale R, Brittle AL, Fisher KH, Monk NA, Strutt D. 2015 Cellular interpretation of the long-range gradient of Four-jointed activity in the *Drosophila* wing. *eLife* **4**, e05789. (doi:10.7554/eLife.05789)
 31. Möröy T, Geisen C. 2004 Cyclin E. *Int. J. Biochem. Cell Biol.* **36**, 1424–1439. (doi:10.1016/j.biocel.2003.12.005)
 32. R Core Team. 2021 *R: a language and environment for statistical computing*. Vienna, Austria: R Foundation for Statistical Computing.
 33. Wickham H *et al.* 2019 Welcome to the tidyverse. *J. Open Sour. Softw.* **4**, 1686. (doi:10.21105/joss.01686)
 34. Wood SN. 2017 *Generalized additive models: An introduction with R*, 2 edn. London, UK: Chapman and Hall.
 35. Lawrence PA, Casal J, Struhl G. 2002 Towards a model of the organisation of planar polarity and pattern in the *Drosophila* abdomen. *Development* **129**, 2749–2760. (doi:10.1242/dev.129.11.2749)
 36. Bosveld F *et al.* 2012 Mechanical control of morphogenesis by Fat/Dachsous/Four-jointed planar cell polarity pathway. *Science* **336**, 724–727. (doi:10.1126/science.1221071)
 37. Mao Y, Rauskolb C, Cho E, Hu WL, Hayter H, Minihan G, Katz FN, Irvine KD. 2006 Dachs: an unconventional myosin that functions downstream of Fat to regulate growth, affinity and gene expression in *Drosophila*. *Development* **133**, 2539–2551. (doi:10.1242/dev.02427)
 38. Rogulja D, Rauskolb C, Irvine KD. 2008 Morphogen control of wing growth through the Fat signaling pathway. *Dev. Cell* **15**, 309–321. (doi:10.1016/j.devcel.2008.06.003)
 39. Ambegaonkar AA, Irvine KD. 2015 Coordination of planar cell polarity pathways through spiny-legs. *eLife* **4**, e09946. (doi:10.7554/eLife.09946)
 40. Pietra S, Ng K, Lawrence PA, Casal J. 2020 Planar cell polarity in the larval epidermis of *Drosophila* and the role of microtubules. *Open Biol.* **10**, 200290. (doi:10.1098/rsob.200290)
 41. Christian JL. 2012 Morphogen gradients in development: from form to function. *Wiley Interdiscip. Rev. Dev. Biol.* **1**, 3–15. (doi:10.1002/wdev.2)
 42. Lawrence PA. 2001 Morphogens: how big is the big picture? *Nat. Cell Biol.* **3**, E151–E154. (doi:10.1038/35083096)
 43. Schamberg S, Houston P, Monk NAM, Owen MR. 2010 Modelling and analysis of planar cell polarity. *Bull. Math. Biol.* **72**, 645–680. (doi:10.1007/s11538-009-9464-0)
 44. Mato JM, Losada A, Nanjundiah V, Konijn TM. 1975 Signal input for a chemotactic response in the cellular slime mold *Dictyostelium discoideum*. *Proc. Natl Acad. Sci. USA* **72**, 4991–4993. (doi:10.1073/pnas.72.12.4991)
 45. Van Haastert PJ. 1983 Sensory adaptation of *Dictyostelium discoideum* cells to chemotactic signals. *J. Cell Biol.* **96**, 1559–1565. (doi:10.1083/jcb.96.6.1559)
 46. Van Haastert PJ, Postma M. 2007 Biased random walk by stochastic fluctuations of chemoattractant-receptor interactions at the lower limit of detection. *Biophys. J.* **93**, 1787–1796. (doi:10.1529/biophysj.107.104356)
 47. Ishikawa HO, Takeuchi H, Haltiwanger RS, Irvine KD. 2008 Four-jointed is a Golgi kinase that phosphorylates a subset of cadherin domains. *Science* **321**, 401–404. (doi:10.1126/science.1158159)
 48. Basler K, Struhl G. 1994 Compartment boundaries and the control of *Drosophila* limb pattern by hedgehog protein. *Nature* **368**, 208–214. (doi:10.1038/368208a0)
 49. Lawrence PA, Struhl G. 1996 Morphogens, compartments, and pattern: lessons from *Drosophila*? *Cell* **85**, 951–961. (doi:10.1016/S0092-8674(00)81297-0)
 50. Merkel M, Sagner A, Gruber FS, Etournay R, Blasse C, Myers E, Eaton S, Julicher F. 2014 The balance of prickle/spiny-legs isoforms controls the amount of coupling between core and fat PCP systems. *Curr. Biol.* **24**, 2111–2123. (doi:10.1016/j.cub.2014.08.005)
 51. Lawrence PA, Struhl G, Casal J. 2008 Do the protocadherins Fat and Dachsous link up to determine both planar cell polarity and the dimensions of organs? *Nat. Cell Biol.* **10**, 1379–1382. (doi:10.1038/ncb1208-1379)
 52. Bando T, Mito T, Maeda Y, Nakamura T, Ito F, Watanabe T, Ohuchi H, Noji S. 2009 Regulation of leg size and shape by the Dachsous/Fat signalling pathway during regeneration. *Development* **136**, 2235–2245. (doi:10.1242/dev.035204)
 53. Zecca M, Struhl G. 2010 A feed-forward circuit linking wingless, Fat-Dachsous signaling, and the Warts-Hippo pathway to *Drosophila* wing growth. *PLoS Biol.* **8**, e1000386. (doi:10.1371/journal.pbio.1000386)
 54. Rovira M, Saavedra P, Casal J, Lawrence PA. 2015 Regions within a single epidermal cell of *Drosophila* can be planar polarised independently. *eLife* **4**, e06303. (doi:10.7554/eLife.06303)
 55. Willecke M, Hamaratoglu F, Sansores-Garcia L, Tao C, Halder G. 2008 Boundaries of Dachsous cadherin activity modulate the Hippo signaling pathway to induce cell proliferation. *Proc. Natl Acad. Sci. USA* **105**, 14 897–14 902. (doi:10.1073/pnas.0805201105)
 56. Matis M, Axelrod JD. 2013 Regulation of PCP by the fat signaling pathway. *Genes Dev.* **27**, 2207–2220. (doi:10.1101/gad.228098.113)
 57. Strutt H, Strutt D. 2021 How do the Fat-Dachsous and core planar polarity pathways act together and independently to coordinate polarized cell behaviours? *Open Biol.* **11**, 200356. (doi:10.1098/rsob.200356)
 58. Ayukawa T, Akiyama M, Mummery-Widmer JL, Stoeger T, Sasaki J, Knoblich JA, Senoo H, Sasaki T, Yamazaki M. 2014 Dachsous-dependent asymmetric localization of spiny-legs determines planar cell polarity orientation in *Drosophila*. *Cell Rep.* **8**, 610–621. (doi:10.1016/j.celrep.2014.06.009)
 59. Olofsson J, Sharp KA, Matis M, Cho B, Axelrod JD. 2014 Prickle/spiny-legs isoforms control the polarity of the apical microtubule network in planar cell polarity. *Development* **141**, 2866–2874. (doi:10.1242/dev.105932)

60. Sharp KA, Axelrod JD. 2016 Prickle isoforms control the direction of tissue polarity by microtubule independent and dependent mechanisms. *Biol. Open* **5**, 229–236. (doi:10.1242/bio.016162)
61. Casal J, Ibáñez-Jiménez B, Lawrence PA. 2018 Planar cell polarity: the *prickle* gene acts independently on both the Ds/Ft and the Stan/Fz systems. *Development* **145**, dev168112. (doi:10.1242/dev.168112)
62. Strutt H, Warrington SJ, Strutt D. 2011 Dynamics of core planar polarity protein turnover and stable assembly into discrete membrane subdomains. *Dev. Cell* **20**, 511–525. (doi:10.1016/j.devcel.2011.03.018)
63. Lawrence PA, Casal J, Struhl G. 2004 Cell interactions and planar polarity in the abdominal epidermis of *Drosophila*. *Development* **131**, 4651–4664. (doi:10.1242/dev.01351)
64. Chorro A, Verma B, Homfeldt M, Ibáñez B, Lawrence PA, Casal J. 2022 Research data supporting 'Planar cell polarity: intracellular asymmetry and supracellular gradients of Dachsous'. *Univers. Cambrid. Open Access Rep.* (doi:10.17863/CAM.85748)
65. Chorro A, Verma B, Homfeldt M, Ibáñez B, Lawrence PA, Casal J. 2022 Data from: Planar cell polarity: intracellular asymmetry and supracellular gradients of Dachsous. Figshare. (doi:10.6084/m9.figshare.c.6238129)